Applied Catalysis B: Environmental 217 (2017) 429–436

Contents lists available at ScienceDirect

Applied Catalysis B: Environmental

journal homepage: www.elsevier.com/locate/apcatb

In-situ synthesis of CoP co-catalyst decorated $Zn_{0.5}Cd_{0.5}S$ photocatalysts with enhanced photocatalytic hydrogen production activity under visible light irradiation

Dongsheng Dai [a,b], Hao Xu [b], Lei Ge [a,b,*], Changcun Han [b], Yangqin Gao [b], Songsong Li [b], Yan Lu [b]

[a] State Key Laboratory of Heavy Oil Processing, College of Science, China University of Petroleum Beijing, No. 18 Fuxue Rd., Beijing 102249, PR China
[b] Department of Materials Science and Engineering, College of Science, China University of Petroleum Beijing, No. 18 Fuxue Rd., Beijing 102249, PR China

ARTICLE INFO

Article history:
Received 6 March 2017
Received in revised form 31 May 2017
Accepted 5 June 2017
Available online 13 June 2017

Keywords:
$Zn_{0.5}Cd_{0.5}S$ nanorods
Photocatalyst
CoP
Water splitting
Visible light

ABSTRACT

The generation of hydrogen (H_2) through photocatalytic water splitting with the employment of various co-catalysts has attracted much attention. In this study, the CoP was successfully decorated on $Zn_{0.5}Cd_{0.5}S$ as a highly efficient co-catalyst via a two-step in-situ chemical deposition method. The chemical as well as photophysical properties of the as-obtained CoP/$Zn_{0.5}Cd_{0.5}S$ samples were characterized by X-ray diffractometry (XRD), Transmission electron microscope (TEM), UV–vis diffusion reflectance spectroscopy (DRS), X-ray photoelectron spectroscopy (XPS) and surface photovoltage spectroscopy (SPV). The CoP/$Zn_{0.5}Cd_{0.5}S$ composite sample with 5% molar content showed the highest photocatalytic H_2 evolution activity with a corresponding H_2 evolution rate of 734 umol h^{-1}, which was about 20 times higher than that of pure $Zn_{0.5}Cd_{0.5}S$ sample and 2 times higher than Pt loaded $Zn_{0.5}Cd_{0.5}S$ sample under visible light irradiation. The photocatalytic activity of the CoP/$Zn_{0.5}Cd_{0.5}S$ composite sample was stable even after 4 cycling photocatalytic experiments. A possible mechanism on the photocatalytic enhancement of CoP was systematically investigated, which can provide a novel concept for the synthesis of other desirable photocatalytic materials with high photocatalytic performance.

1. Introduction

Hydrogen energy has received growing attention as a renewable and environmental friendly fuel due to the aggravating energy crisis and environmental problems [1–3]. Since Honda and Fujishima discovered the photocatalytic water splitting on TiO_2 in 1972 [4], several investigations are focused on the application of semiconductors such as oxides, oxynitrides, and metal sulfides in H_2 evolution through water splitting with utilization of solar energy [5–12]. However, large bandgap semiconductors such as TiO_2 and ZnO could only respond to light in UV range, which contains only about 4% of solar energy, and directly limit their application to a great extent [13–15]. Therefore, it remains a major challenge to develop efficient visible light photocatalysts in the field of photot-catalysts.

Recently, metal sulfide semiconductors have received considerable attention for photocatalytic H_2 evolution due to their appropriate bandgap and catalytic properties [16–20]. Among them, cadmium sulfide (CdS) has gained intensive interest for its visible light responding band gap, 2.49 eV. However, rapid recombination kinetics of photoexcited electron-hole pairs and serious photo-corrosion result in low quantum efficiencies which limit its photocatalytic performance. Constructing ternary metal sulfides such as $Cd_xZn_{1-x}S$ provides a promising strategy to enhance the photocatalytic performance of CdS. It has been reported that $Cd_xZn_{1-x}S$ is a good candidate in H_2 production under visible light [20,21]. More importantly, $Cd_xZn_{1-x}S$ exhibits superior photocatalytic performance than CdS and ZnS. Although the photocatalytic behaviors of $Cd_xZn_{1-x}S$ have been investigated, serious problem of rapid recombination of electrons and holes still present and should be resolved to further improve its photocatalytic performance. Co-catalysts have been demonstrated to be an efficient way in enhancing the photocatalytic activity and stability of photocatalysts, which mainly arise from their capability in suppressing the charge carrier recombinations. Currently, noble metals have been proven to be a high performance co-catalyst because of their

* Corresponding author at: State Key Laboratory of Heavy Oil Processing, China University of Petroleum Beijing, No. 18 Fuxue Road, Beijing 102249, PR China.
E-mail address: gelei08@sina.com (L. Ge).

http://dx.doi.org/10.1016/j.apcatb.2017.06.014
0926-3373/

high work functions and low overpotentials for hydrogen evolution [22–27]. However, noble metals are usually rare elements and possess high-cost, which is detrimental for large-scale applications. Therefore, it is highly desired to find an earth-abundant and inexpensive alternative for noble metals.

Numerous noble-metal-free materials have been studied as co-catalysts in the past several decades, such as transition metals [28,29], carbon-based materials [30,31], hydroxides [32–34], transition metal oxides [35–37], and sulfides [38,39], etc. Recently, several groups have shown that transition-metal phosphides, such as Ni_2P [40], Cu_3P [41], CoP [42] and FeP [43], can be used as co-catalyst to effectively increase the catalytic performance of photocatalysts. Compare to other noble-metal-free co-catalysts mentioned above, phosphides exhibit many attractive advantages, including high activity of hydrogen production, reasonable stability, etc. These characteristics of phosphides imply that phosphides could be potentially serve as an efficient noble-metal-free co-catalyst for $Cd_xZn_{1-x}S$ to enhance its photocatalytic performance in the photocatalytic H_2 evolution.

In this study, for the first time CoP decorated $Zn_{0.5}Cd_{0.5}S$ nanorods are synthesized and investigated as a novel photocatalyst for H_2 evolution. The CoP/$Zn_{0.5}Cd_{0.5}S$ hybrid photocatalysts are prepared based on a two-step in-situ chemical deposition and low-temperature treatment method. The structural characteristics and optical properties of CoP/$Zn_{0.5}Cd_{0.5}S$ composite photocatalysts are analyzed. The photocatalytic H_2 evolution activity and stability for CoP/$Zn_{0.5}Cd_{0.5}S$ under visible light irradiation are also characterized. The possible photocatalytic mechanism for enhanced H_2 evolution activity was proposed. The result demonstrates that CoP can act as an effective co-catalyst for $Zn_{0.5}Cd_{0.5}S$ which gives us a revelation that it may be also potentially applied for other semiconductor photocatalysts for H_2 evolution.

2. Experimental

2.1. Materials

zinc nitrate hexahydrate ($Zn(NO_3)_2{\cdot}6H_2O$, Aladdin), cadmium chloride ($CdCl_2{\cdot}2.5H_2O$, Aladdin, 98%), ethylenediamine (A.R), thioacetamide (A.R), sodium hypophosphite (NaH_2PO_2, A.R), cobalt dichloride ($CoCl_2$,Aladdin), NaOH (A.R), poly vinyl alcohol (Aldrich), Sodium borohydride ($NaBH_4$, Aladdin), ethyl alcohol (EtOH, A.R.) and lactic acid (A.R) were used as received without additional purification or treatment. Deionized water was used in all experiments.

2.2. Synthesis of the photocatalysts

The $Zn_{0.5}Cd_{0.5}S$ sample was prepared according to a literature method with a slight modification [44]. A total of 5 mmol equimolar of zinc nitrate hexahydrate and cadmium chloride were added to 30 mL of ethylenediamine followed with another addition of 20 mmol thioacetamide. After vigorous stirring for 1 h at room temperature, the white solution was transferred to a 50 mL capacity Teflon-lined stainless steel autoclave and heated at 180 °C for 24 h. After that, the product was washed by centrifugation with distilled water and ethanol for several times, respectively. Finally, the final product was obtained via drying the washed solution under vacuum at 60 °C overnight.

The CoP/$Zn_{0.5}Cd_{0.5}S$ composite catalysts were synthesized by a simple two-step in-situ reaction method [45]. At first, 2 mmol $Zn_{0.5}Cd_{0.5}S$ nanorods was dispersed in 100 mL water, and a certain amount of $CoCl_2$ was added according to designated molar ratio. After vigorous stirring for half an hour, an excess of 0.5 M NaOH was slowly added and stirred for another 4 h at room temperature. Then the collected precipitate was washed by centrifugation with water and ethanol for three times and dried under vacuum at 60 °C overnight. Secondly, the previously obtained precipitate was placed in a crucible together with NaH_2PO_2, and the whole crucible was put into a tube furnace at room temperature with an orientation that the precipitate was located at the downstream side. The furnace was first heated from room temperature to 250 °C in 30 min, and then slowly ramped to 350 °C with a rate of 1 °C/min, and kept at 350 °C for 2 h in the atmosphere of Ar (50 sccm). Finally, CoP/Cd0.5Zn0.5S composite samples with different molar contents were obtained. The molar percentages of CoP in the prepared composite catalyst were 0.5%, 1%, 3%, 5%, 7% and 9%, respectively.

The deposition of Pt on $Zn_{0.5}Cd_{0.5}S$ was carried out by the following experimental method [23]: 10 mM $H_2PtCl_6{\cdot}3H_2O$, 0.1 M $NaBH_4$ and 1.0 wt% poly vinyl alcohol (PVA) aqueous solution were prepared as stock solutions. The as-prepared $Zn_{0.5}Cd_{0.5}S$ nanorods (0.1 g) were dispersed in 50 mL distilled water to form homogeneous suspension under continuous stirring. Then the $H_2PtCl_6{\cdot}3H_2O$ stock solution and an appropriate amount of PVA solution was added (PVA/Pt = 1.2, weight ratio). After that, the fresh $NaBH_4$ solution ($NaBH_4$/(Pt) = 5, molar ratio) was also added. After stirring for 1 h at room temperature, the products were washed by centrifugation with deionized water and ethanol for three times, respectively, then dried under vacuum at 60 °C overnight.

2.3. Characterization

The X-ray diffractometer (XRD) using Cu Kα as radiation was applied to investigate the crystallographic texture of all samples with 2θ ranges from 20° to 65°. The morphology of all samples was identified by transmission electron microscopy (TEM, JEM-2100, accelerating voltage 200 kV). The UV–vis diffuse reflection spectroscopy (DRS) of all samples was detected by Shimadzu UV-4100 spectrophotometer, and $BaSO_4$ was used as a reflectance standard. X-ray photoelectron spectroscopy (XPS, PHI 5300 ESCA system) was applied to analyze the element valence state of the composite sample, the signal of carbon at 284.8 eV was used as a reference to calibrate the binding energies.

2.4. Photocatalytic activity

The photocatalytic H_2 evolution was carried out in a 300 mL quartz reactor (Perfectlight Labsolar IIAG system), connected with a low-temperature thermostat bath to keep the reaction temperature at 4 °C during the characterization. A 300 W xenon arc lamp with a 420 nm cut-off filter (PLS-SXE 300UV) was used to simulate the visible light source. The illumination intensity was adjusted to 11.0 mW/cm^2. In a typical photocatalytic H_2 evolution experiment process, 50 mg of catalysts was dispersed in 100 mL of mixed aqueous solution containing 90 mL water and 10 mL sacrificial agent (lactic acid) with constant stirring. Before photocatalytic experiments, the reaction system was evacuated for 30 min to create an anaerobic condition. A gas chromatography (Beifen 3420 A, TCD) was selected to analyze the products, and high purity Argon was utilized as carrier gas.

2.5. SPV measurements

The surface photovoltage (SPV) measurement was carried out on a surface photovoltage spectroscopy (PL-SPS/IPCE1000 Beijing Perfect Light Technology Co, Ltd). The measurement system is composed of a source of monochromatic light, a lock-in amplifier (SR830, Stanford research systems, Inc.), a light chopper (SR 540, Stanford research systems, Inc.), and a sample cell, respectively. The entire measurement was operated under ambient condition.

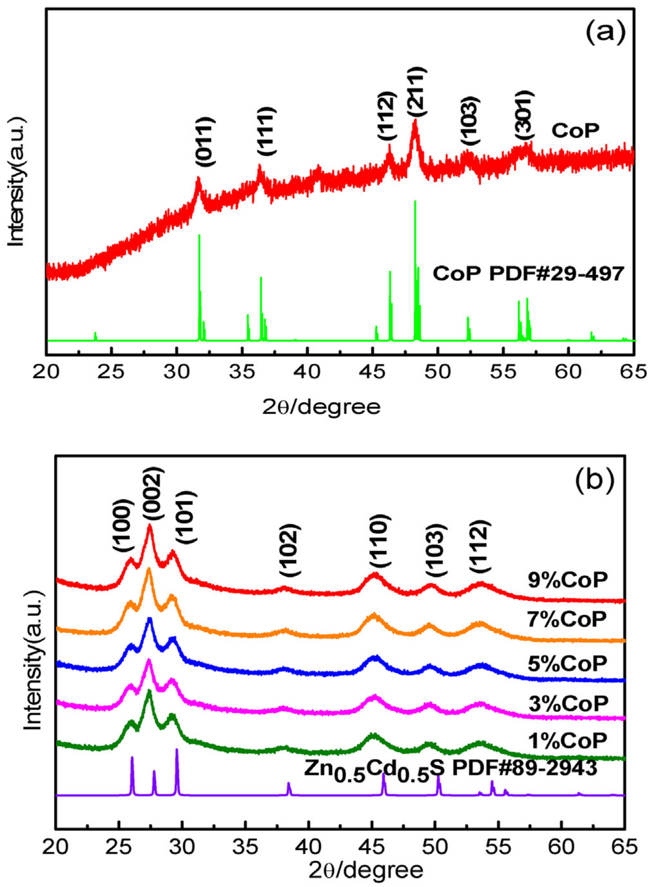

Fig. 1. XRD patterns of pure CoP(a), CoP/$Zn_{0.5}Cd_{0.5}S$ composites(b) with different weight ratios of CoP.

3. Results and discussion

3.1. Characterization of CoP/$Zn_{0.5}Cd_{0.5}S$ composite samples

The phase purity and crystal structure of as-prepared products was first characterized by XRD analysis. The XRD patterns of as-prepared CoP are demonstrated in Fig. 1(a). Typical diffraction peaks corresponding to CoP (2θ = 31.68°, 36.41°, 46.32°, 48.21°, 52.31°, 56.86°) are observed, which are in good agreement with (011), (111), (112), (211), (103) and (301) of orthorhombic CoP in JCPDS No. 29-497 respectively. The representative XRD patterns of CoP/$Cd_{0.5}Zn_{0.5}S$ are shown in Fig. 1(b), data of the standard card of hexagonal $Zn_{0.5}Cd_{0.5}S$ (JCPDS No. 89-2943) are also shown as reference. The main peaks of 2θ at 26.11°, 27.76°, 29.62°, 38.49°, 46.02°, 50.25° and 54.58° can be readily indexed to the (100), (002), (101), (102), (110), (103) and (112) planes of hexagonal $Zn_{0.5}Cd_{0.5}S$, respectively. It is obvious that deposition of CoP did not affect the crystal structure of $Zn_{0.5}Cd_{0.5}S$. However, no apparent diffraction peaks of CoP were observed in all composite samples, which may indicates that the CoP depositing content in CoP/$Zn_{0.5}Cd_{0.5}S$ is low and insensitive for XRD characterization. Nevertheless, the presence of CoP in the composites can be easily proved by TEM and XPS techniques as will be discussed later.

TEM was further applied to investigate the microstructures of $Zn_{0.5}Cd_{0.5}S$ and CoP/$Zn_{0.5}Cd_{0.5}S$ composite samples. As shown in Fig. 2(a), it can be seen that the pure $Zn_{0.5}Cd_{0.5}S$ sample has a rod-like morphology with diameter of 80 nm~ 120 nm. After the chemical reduction deposition of CoP on $Zn_{0.5}Cd_{0.5}S$, CoP was deposited as nanoparticles on the $Zn_{0.5}Cd_{0.5}S$ surface with high dispersion, and there is no obvious change in the microstructure of $Zn_{0.5}Cd_{0.5}S$ nanorods (Fig. 2(c)). Fig. 2(b) and (d–f) present the HRTEM images of the $Zn_{0.5}Cd_{0.5}S$ sample and CoP/$Zn_{0.5}Cd_{0.5}S$ composite, different orientations and interplanar spacing was revealed. The identified lattice fringes of 0.32 nm corresponds to the (002) lattice plane of $Zn_{0.5}Cd_{0.5}S$ phase. In addition, an interplanar spacing of 0.19 nm can be seen which was ascribed to CoP [46]. Fig. 3 displays the elemental distribution maps (Zn, Cd, S, Co and P respectively), the result of CoP/$Zn_{0.5}Cd_{0.5}S$ shows that elements of Zn, Cd, S, Co and P can be clearly observed. It is found that Zn, Cd, S, Co and P elements distribute almost uniformly in the surface of CoP/$Zn_{0.5}Cd_{0.5}S$, which further confirmed the CoP/$Zn_{0.5}Cd_{0.5}S$ composite photocatalysts were prepared successfully. The TEM results indicate that close contacted interfaces are formed between CoP and $Zn_{0.5}Cd_{0.5}S$ components in the composite sample, which could serve as a role for effective improvement of the separation efficiency of photogenerated electrons-holes.

The UV–vis diffuse reflectance spectra (DRS) of as-prepared $Zn_{0.5}Cd_{0.5}S$ and CoP/$Zn_{0.5}Cd_{0.5}S$ composite samples were performed to determine their light-absorbing ability. As shown in Fig. 4, the pure $Zn_{0.5}Cd_{0.5}S$ sample shows absorption from UV to the visible range with an abrupt decline at ~500 nm, indicating that the visible light absorption is ascribed to the band gap transition [23]. The band gap value of $Zn_{0.5}Cd_{0.5}S$ is about 2.48 eV determined by Tauc's plot as shown in Fig. 4 insert, which is consistent with the value reported previously [49]. After introduction of CoP co-catalyst, the CoP/$Zn_{0.5}Cd_{0.5}S$ samples show a similar absorption edge in shape and exhibit remarkably improved light absorption intensity compared with pure $Zn_{0.5}Cd_{0.5}S$ in the visible region. The absorption intensity of the as-prepared samples is strengthened with increasing CoP contents, which agrees with the color of the prepared samples that vary from light yellow to dark gray. However, if excessive CoP co-catalysts are introduced, CoP NPs may cover on the surface of $Zn_{0.5}Cd_{0.5}S$, and will compete with $Zn_{0.5}Cd_{0.5}S$ to adsorb the visible light, which can inhibit the light absorption of $Zn_{0.5}Cd_{0.5}S$ photocatalysts and may have negative effect on the photocatalytic activity [24,50]. The DRS results further confirm that the chemical in-situ deposited CoP has considerable effect for efficient utilization of visible light.

The X-ray photoelectron spectroscopy (XPS) analysis was explored in order to gain deeper insight into the surface deposition of CoP/$Zn_{0.5}Cd_{0.5}S$ sample. Fig. 5(f) presents the survey spectrum of the CoP/$Zn_{0.5}Cd_{0.5}S$ sample, which proves the co-existence of Zn, Cd, S, Co and P elements as expected. In the Zn 2p and Cd 3d XPS spectra (Fig. 5(a) and (b)), the binding energies of Zn 2p (1021.7 eV and 1044.8 eV) and Cd 3d (405.0 eV and 411.7 eV) agree well with the values reported in the previous work [24]. The S 2p XPS binding energy can be divided into three peaks located at 161.3 eV, 161.6 eV and 162. 6 eV, which can be assigned to the S^{2-} state [24]. As shown in Fig. 5d, The Co 2p peaks located at 778.3 eV and 793.7 eV are in accordance with the Co $2p_{3/2}$ and Co $2p_{1/2}$ in the CoP. Meanwhile, as shown in Fig. 5e, the peak at 129.7 eV which belongs to the P(2p) species in CoP is negatively shifted compared to that of elemental P (130.2 eV) [45,46]. The shifts of the binding energies (BE) of Co(2p) and P(2p) regions indicate that Co carries a partial positive charge (δ^+) while P has a partial negative charge (δ^-). The binding energy at 133.8 eV is ascribed to oxidized P species due to the superficial oxidation of CoP upon exposing to air [46].

3.2. Photocatalytic H_2 evolution activity

The photocatalytic H_2 evolution activities of CoP/$Zn_{0.5}Cd_{0.5}S$ and comparative samples were shown in Fig. 6. The control experiment of H_2 evolution evaluation over pure CoP sample is also carried out; the result shows that the pure CoP sample shows no H_2 evolution activity. The pure $Zn_{0.5}Cd_{0.5}S$ sample without CoP exhibited a photocatalytic H_2 production activity of 37 umol h^{-1}. After intro-

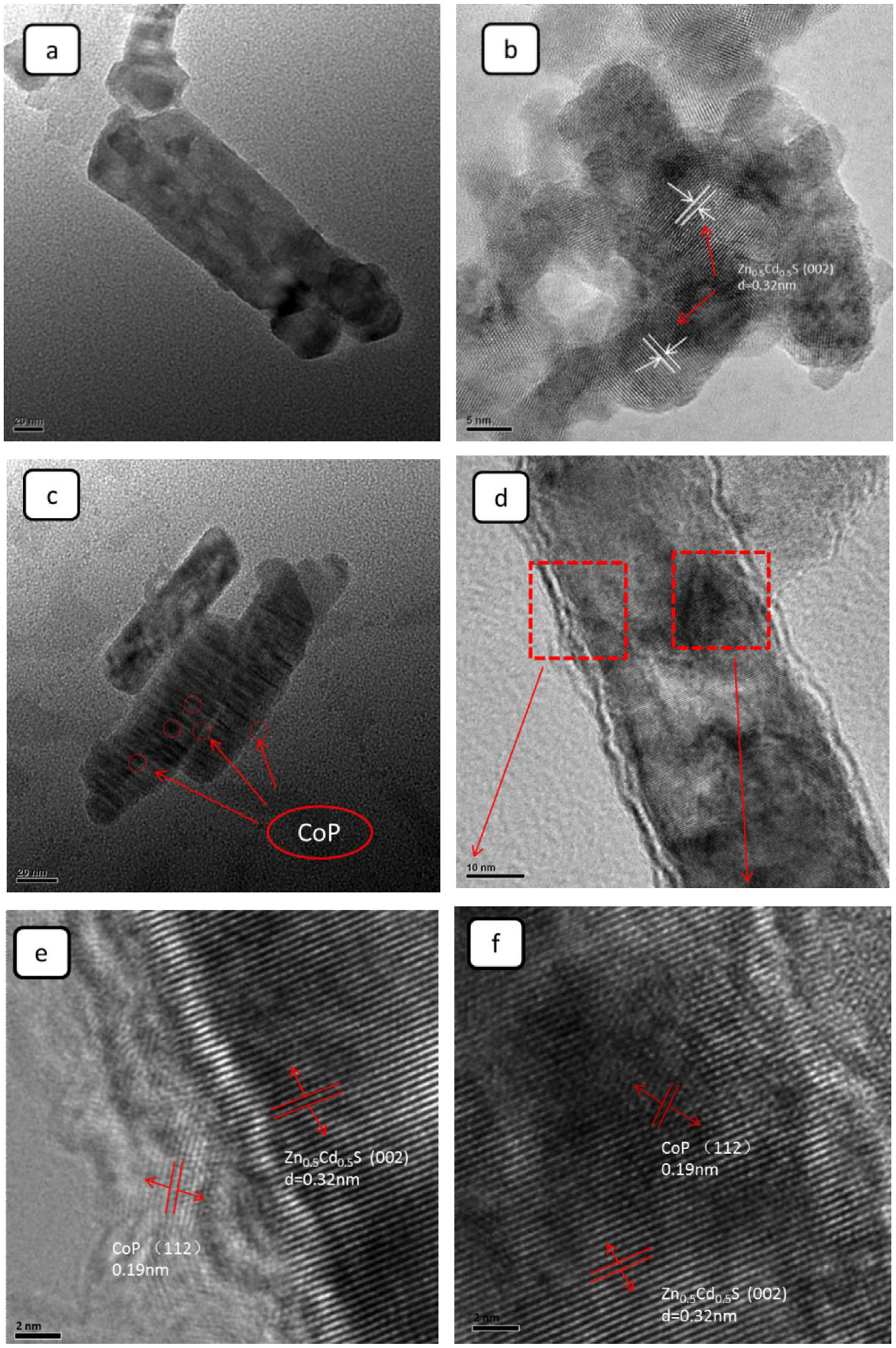

Fig. 2. TEM images of $Zn_{0.5}Cd_{0.5}S$ sample (a), CoP/$Zn_{0.5}Cd_{0.5}S$ composite (c, d); HRTEM image of $Zn_{0.5}Cd_{0.5}S$ sample (b), CoP/$Zn_{0.5}Cd_{0.5}S$ composite (e,f).

ducing of CoP, the activity of photocatalytic hydrogen production is significantly enhanced. Fig. 7 presents the H_2 evolution rate of CoP/$Zn_{0.5}Cd_{0.5}S$ composite samples with different CoP contents. After loading 0.5% CoP on $Zn_{0.5}Cd_{0.5}S$ nanorods, the H_2 evolution activity is remarkably increased to 281 umol h^{-1}. Along with the increase of CoP amounts, the H_2 evolution is further improved. The 5% CoP/$Zn_{0.5}Cd_{0.5}S$ sample presents the highest H_2 evolution activity with a H_2 evolution rate of 734 umol h^{-1}, which is 20 times higher than that of pure $Zn_{0.5}Cd_{0.5}S$ and 2 times higher than that shown in Pt decorated $Zn_{0.5}Cd_{0.5}S$. Meanwhile, the results shown in Fig. 7 indicate that the photocatalytic activity of the simple mechanical mixture of CoP particles and $Zn_{0.5}Cd_{0.5}S$ nanorods is much weaker than that of CoP/$Zn_{0.5}Cd_{0.5}S$, the enhanced photocatalytic performance may be attributed to the intimate interfaces between CoP and $Zn_{0.5}Cd_{0.5}S$, which can effectively promote the separation efficiency of the photo-generated electron-hole pairs. However, a further increase of CoP content leads to a decrease in H_2 evolution rate. The decrease in the photocatalytic activity may be due to the high loading ratio of black CoP, which can inhibit the incident light absorption of $Zn_{0.5}Cd_{0.5}S$, leading to decreasing the number of photo generated electrons [47]. Moreover, the DRS results show that the excessive CoP will compete with $Zn_{0.5}Cd_{0.5}S$ to adsorb the

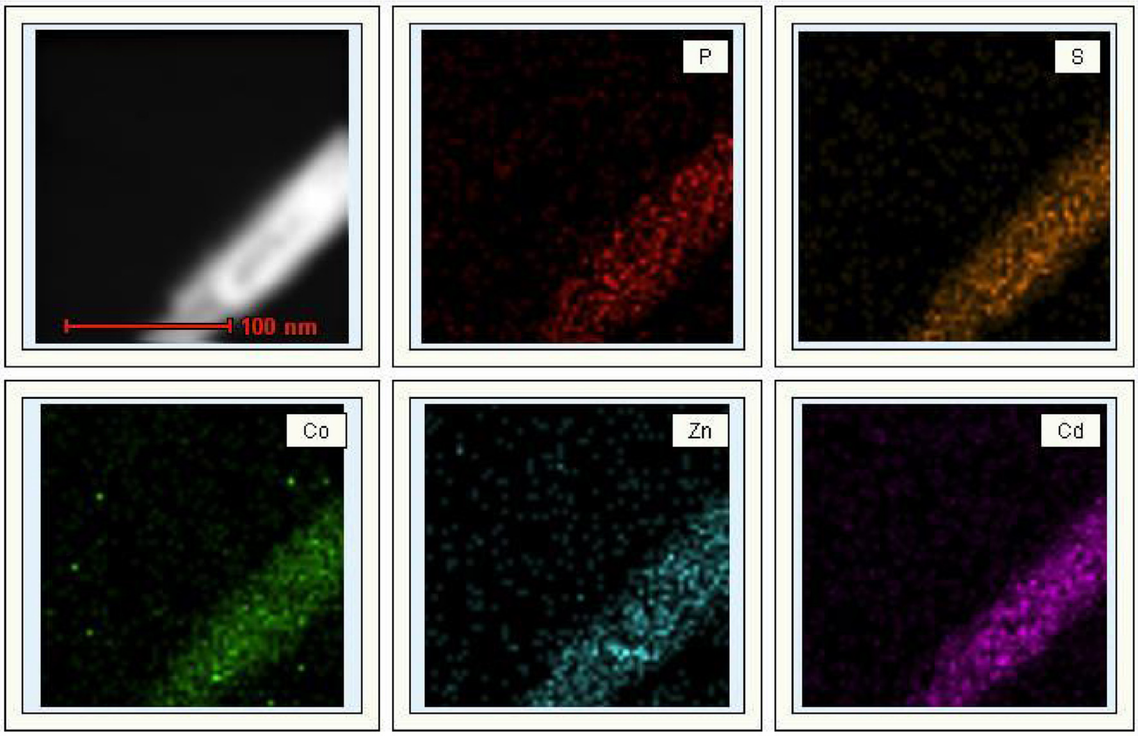

Fig. 3. TEM mapping of 5% CoP/$Cd_{0.5}Zn_{0.5}S$ composite.

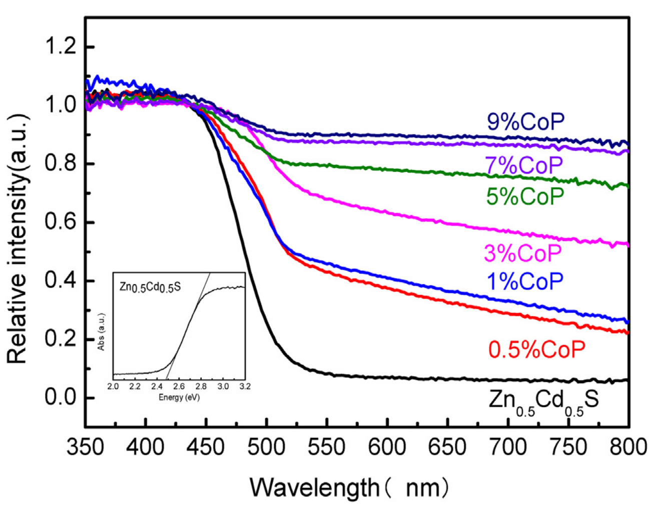

Fig. 4. UV–vis diffuse reflectance spectra of pure $Zn_{0.5}Cd_{0.5}S$, and CoP/$Zn_{0.5}Cd_{0.5}S$ composites with different molar ratios of CoP.

visible light. Thus, the competition of light absorption should be another key parameter leading to decrease of H_2 evolution rate. Therefore, a suitable amount of CoP is important for optimization of the photocatalytic activity of CoP/$Zn_{0.5}Cd_{0.5}S$ composite samples. Fig. 8 illustrates the photocatalytic H_2 evolution activities of $Zn_xCd_{1-x}S$ and CoP/$Zn_xCd_{1-x}S$ samples. After loading 5% CoP co-catalyst on $Zn_xCd_{1-x}S$ nanorods, and all samples show significantly improved photocatalytic hydrogen production activity.

The stability of a photocatalyst is highly critical for its practical applications. The catalytic stability of the 5% CoP/$Zn_{0.5}Cd_{0.5}S$ sample was further investigated via cycling experiments of photocatalytic H_2 evolution. Fig. 9 illustrates the H_2 evolution curves in cycling photocatalytic run. The H_2 production does not display obvious decrease after irradiated for 16 h (4 cycles), which indicates that the CoP/$Zn_{0.5}Cd_{0.5}S$ photocatalyst has sufficient stability for photocatalytic H_2 production.

3.3. Photocatalytic mechanism investigation

Based on the microstructure characterizations and the visible light photocatalytic performance of CoP/$Zn_{0.5}Cd_{0.5}S$, a possible mechanism for photocatalytic H_2 evolution of the CoP/$Zn_{0.5}Cd_{0.5}S$ catalyst is proposed. As illustrated in Fig. 10, $Zn_{0.5}Cd_{0.5}S$ absorbs photons and excites electron-hole pairs under visible-light irradiation. However, without the co-catalyst, the photo-generated electrons and holes are likely to recombine rapidly which results in a low photocatalytic H_2 production activity. As the conduction band edge and valance band edge of CoP are determined to be −0.43 eV and 1.3 eV [45,48] and the conduction band edge and valance band edge of $Zn_{0.5}Cd_{0.5}S$ locate at −1.06 eV and 1.42 eV [49], respectively. However, the pure CoP NPs act only as cocatalyst and show no photocatalytic H_2 evolution activity in this study. After introduce of CoP co-catalyst, the CoP NPs show higher electron-capture capability due to their low Fermi level so that photo-generated electrons can be stimulated to quickly transfer from the conduction band (CB) of $Zn_{0.5}Cd_{0.5}S$ towards CoP surface, leading to efficient separation of the photoexcited hole-electron pairs. It also indicates that CoP NPs can act as electron collector and transporter to prolong the lifetime of the charge carriers, thus enhancing the photocatalytic activity [45]. In addition, the CoP and $Zn_{0.5}Cd_{0.5}S$ can closely bound together and form intimate interfaces, which can offer a larger active surface area and maximize the electrons transfer efficiency. The holes in the valence band (VB) of $Zn_{0.5}Cd_{0.5}S$ are captured and consumed by lactic acid sacrificial regents.

To further verify the mechanism, surface photovoltage characterization (SPV), a powerful technique for investigating the separation of carriers, is performed. Fig. 11 presents the SPV spectra of pure $Zn_{0.5}Cd_{0.5}S$ and CoP/$Zn_{0.5}Cd_{0.5}S$ nanorods composites with different molar ratios of CoP. The results indicate that all samples show a strong response at the wavelength region from 300 nm

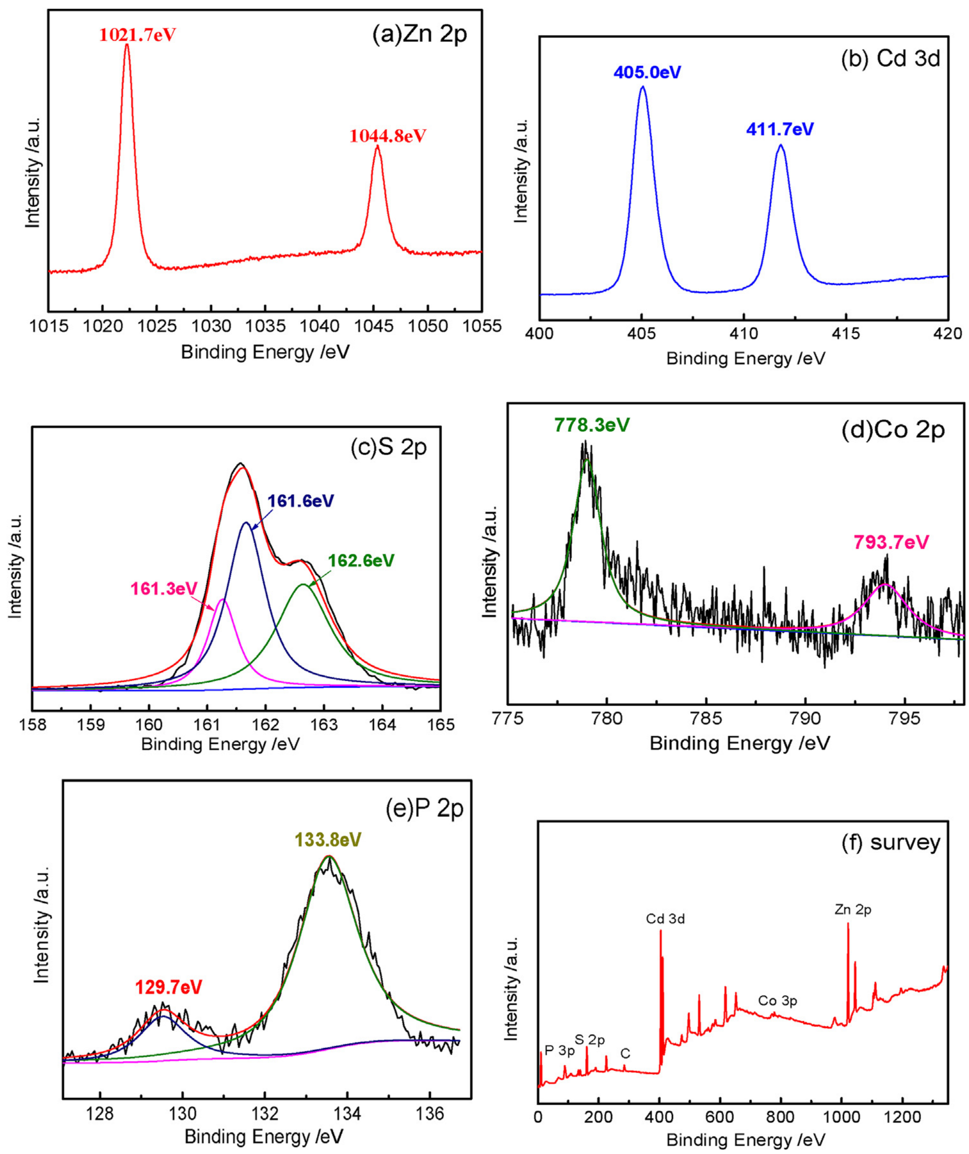

Fig. 5. XPS spectra of CoP/$Zn_{0.5}Cd_{0.5}S$ samples: (a) Zn 2P; (b) Cd 2d; (c) S 2p; (d) Co 2p;(e)P 2p;(f) survey.

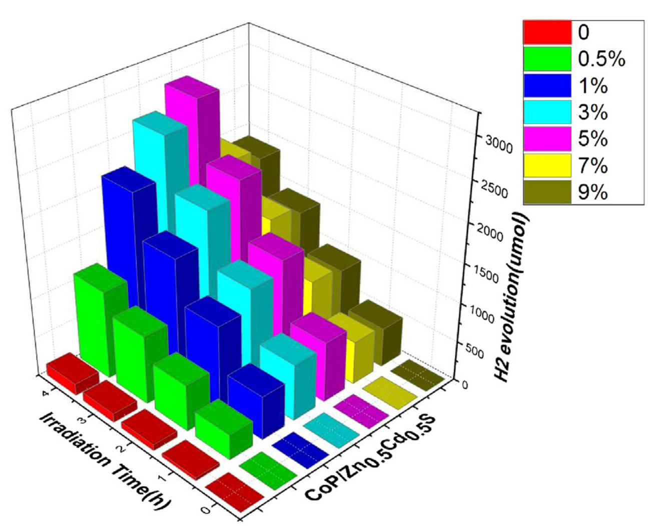

Fig. 6. Photocatalytic H_2 evolution over CoP/$Zn_{0.5}Cd_{0.5}S$ composite samples with different CoP contents under visible light.

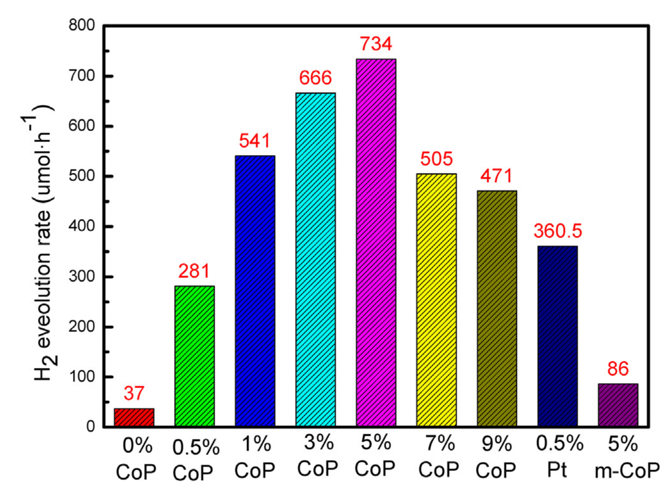

Fig. 7. Rate of H_2 evolution over CoP/$Zn_{0.5}Cd_{0.5}S$ composite samples with different CoP contents, Pt/$Zn_{0.5}Cd_{0.5}S$ and m-CoP/$Zn_{0.5}Cd_{0.5}S$ (simple mechanical mixture CoP particles and $Zn_{0.5}Cd_{0.5}S$ nanorods).

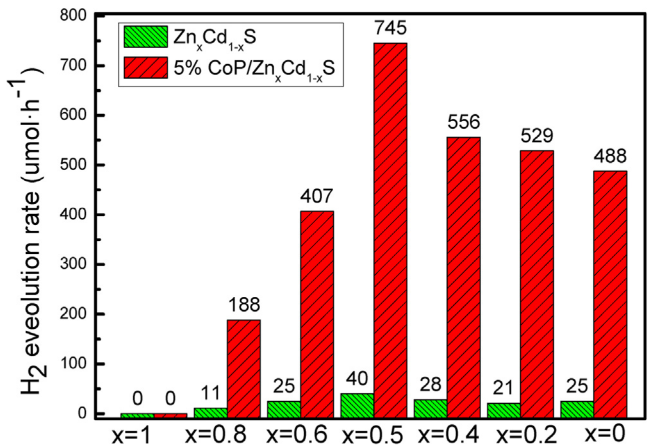

Fig. 8. Rate of H_2 evolution $Zn_xCd_{1-x}S$ and over 5% CoP/$Zn_xCd_{1-x}S$ composite samples.

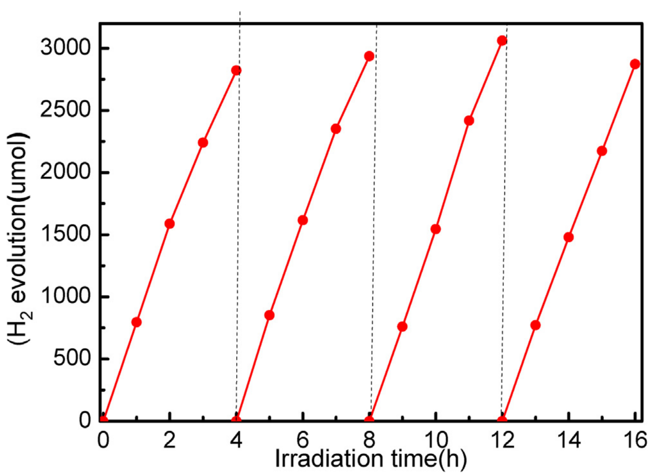

Fig. 9. Cycling runs for the photocatalytic H_2 evolution in the presence of the 5% CoP/$Zn_{0.5}Cd_{0.5}S$ composite sample under visible light irradiation.

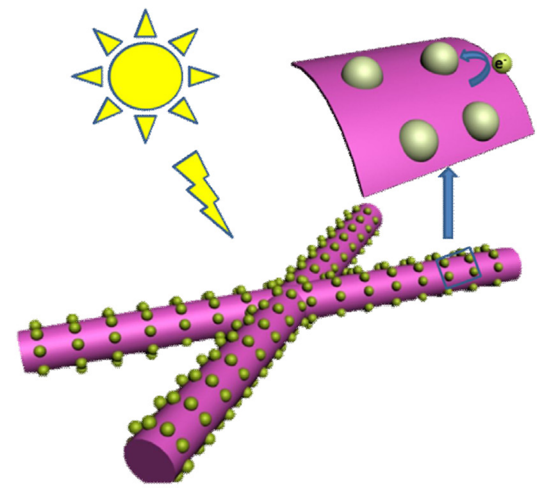

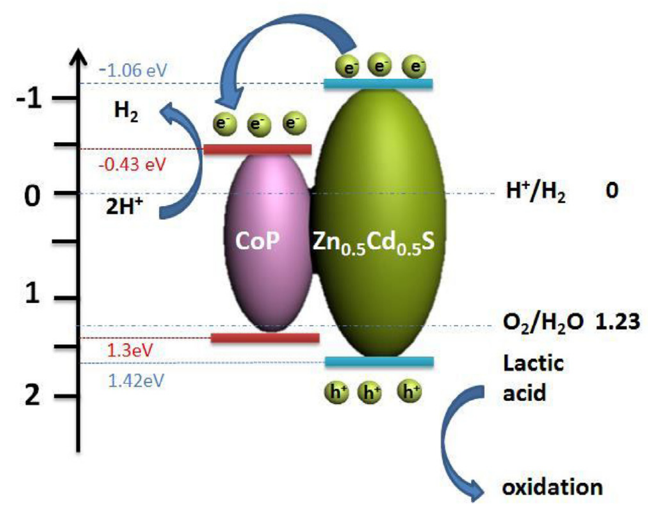

Fig. 10. Schematic illustration for the charge transfer and separation in CoP/$Zn_{0.5}Cd_{0.5}S$ system and proposed mechanism for photocatalytic H_2 production under visible light irradiation.

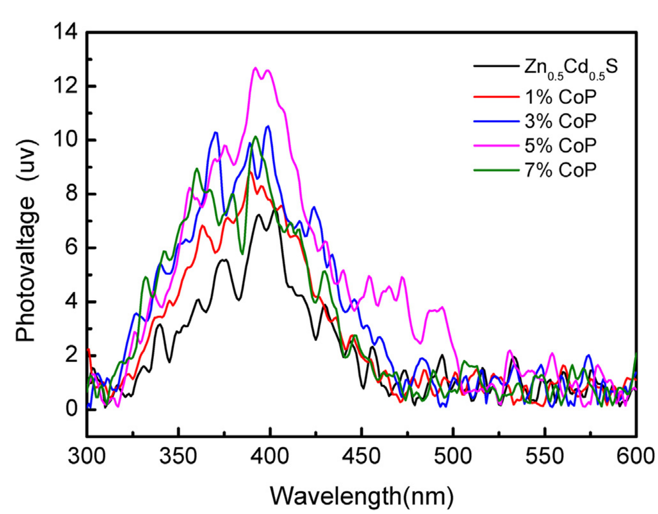

Fig. 11. SPV spectra of pure $Zn_{0.5}Cd_{0.5}S$ and CoP/$Zn_{0.5}Cd_{0.5}S$ composites with different molar ratios of CoP.

to 500 nm, which corresponds with the band gap of $Zn_{0.5}Cd_{0.5}S$. In addition, the 5%CoP/$Zn_{0.5}Cd_{0.5}S$ composite sample shows a much stronger response than that of pure $Zn_{0.5}Cd_{0.5}S$, indicating that the separation efficiency of charge carriers in composite samples is much higher than that in pure $Zn_{0.5}Cd_{0.5}S$ [23]. However, if excessive CoP is introduced, the light absorption by $Zn_{0.5}Cd_{0.5}S$ is reduced as excess CoP NPs prevent the light absorption from reaching the $Zn_{0.5}Cd_{0.5}S$ surface, which leads to a decrease of the SPV signal in comparison to that of the 5% CoP/$Zn_{0.5}Cd_{0.5}S$ sample. The results of SPV spectra and photocatalytic H_2 evolution illustrate that the band alignment and tight interface present between CoP and $Zn_{0.5}Cd_{0.5}S$ nanorods plays an important role in charge carriers separation, which promote the transition of electrons from $Zn_{0.5}Cd_{0.5}S$ to CoP, and in turns enhance the photocatalytic activity of $Zn_{0.5}Cd_{0.5}S$.

4. Conclusions

In summary, a highly efficient composite and noble-metal-free photocatalysts CoP/$Zn_{0.5}Cd_{0.5}S$ were prepared based on a two-step in-situ chemical deposition method. The CoP NPs are dispersed uniformly on the surface of $Zn_{0.5}Cd_{0.5}S$ nanorods and form intimate contact interfaces. A highest H_2 amount as high as 734 umol h^{-1} was obtained in 5%-CoP/$Zn_{0.5}Cd_{0.5}S$ sample, which was 20 times than that for pure $Zn_{0.5}Cd_{0.5}S$ and 2 times higher than that for Pt loaded $Zn_{0.5}Cd_{0.5}S$. In addition, the 5%-CoP/$Zn_{0.5}Cd_{0.5}S$ sample exhibited a good stability in time-circle experiments. Finally, a

possible photocatalytic mechanism of suppressed charge recombination and promoted charge transition at the CoP/$Zn_{0.5}Cd_{0.5}S$ interface is proposed to explain the observed H_2 evolution activity enhancement in CoP decorated $Zn_{0.5}Cd_{0.5}S$ sample, which was later confirmed by the surface photovoltage (SPV) technique. Therefore, the results illustrate that CoP is a promising co-catalyst for $Zn_{0.5}Cd_{0.5}S$, which can be also potentially used in photocatalytic H_2 production process for other photocatalysts.

Acknowledgements

This work was financially supported by the National Science Foundation of China (Grant No. 51572295, 21003157 and 21273285), Beijing Nova Program (Grant No. 2008B76), and Science Foundation of China University of Petroleum, Beijing (Grant No. KYJJ2012-06-20 and 2462016YXBS05).

References

[1] X. Feng, S. Maier, M. Salmeron, J. Am. Chem. Soc. 134 (2012) 5662–5668.
[2] M.R. Hoffmann, S.T. Martin, W. Choi, D.W. Bahnemann, Chem. Rev. 95 (1995) 69–96.
[3] A. Kudo, Y. Miseki, Chem. Soc. Rev. 38 (2009) 253–278.
[4] A. Fujishima, K. Honda, Nature 238 (1972) 37–38.
[5] X. Zeng, Z. Wang, N. Meng, D.T. McCarthy, A. Deletic, J.-H. Pan, X. Zhang, Appl. Catal. B 202 (2017) 33–41.
[6] T. Xu, L. Zhang, H. Cheng, Y. Zhu, Appl. Catal. B 101 (2011) 382–387.
[7] Z. Wang, J. Hou, C. Yang, S. Jiao, K. Huang, H. Zhu, Energy Environ. Sci. 6 (2013) 2134–2144.
[8] A. Enesca, M. Baneto, D. Perniu, L. Isac, C. Bogatu, A. Duta, Appl. Catal. B 186 (2016) 69–76.
[9] J. Wen, X. Li, H. Li, S. Ma, K. He, Y. Xu, Y. Fang, W. Liu, Q. Gao, Appl. Surf. Sci. 358 (2015) 204–212.
[10] J. Wen, X. Li, W. Liu, Y. Fang, J. Xie, Y. Xu, Chin. J. Catal. 36 (2015) 2049–2070.
[11] X. Jia, M. Tahir, L. Pan, Z.-F. Huang, X. Zhang, L. Wang, J.-J. Zou, Appl. Catal. B 198 (2016) 154–161.
[12] X. Li, J. Wang, Y. Men, Z. Bian, Appl. Catal. B 187 (2016) 115–121.
[13] S.G. Kumar, L.G. Devi, J. Phys. Chem. A 115 (2011) 13211–13241.
[14] J.-I. Hong, J. Choi, S.S. Jang, J. Gu, Y. Chang, G. Wortman, R.L. Snyder, Z.L. Wang, Nano. Lett. 12 (2012) 576–581.
[15] F.X. Xiao, ACS Appl. Mater. Interfaces 4 (2012) 7055–7063.
[16] M. Luo, Y. Liu, J. Hu, H. Liu, J. Li, ACS Appl. Mater. Interfaces 4 (2012) 1813–1821.
[17] J. Zhang, J. Yu, Y. Zhang, Q. Li, J.R. Gong, Nano Lett. 11 (2011) 4774–4779.
[18] A. Ivanovskaya, N. Singh, R.-F. Liu, H. Kreutzer, J. Baltrusaitis, T. Van Nguyen, H. Metiu, E. McFarland, Langmuir 29 (2013) 480–492.
[19] Q. Li, X. Li, S. Wageh, A.A. Al-Ghamdi, J. Yu, Adv. Energy. Mater. 5 (2015) 1500010.
[20] K. Iwashina, A. Iwase, Y.H. Ng, R. Amal, A. Kudo, J. Am. Chem. Soc. 137 (2015) 604–607.
[21] L. Zhu, Y. Wang, D. Zhang, C. Li, D. Sun, S. Wen, Y. Chen, S. Ruan, ACS Appl. Mater. Interfaces 7 (2015) 20793–20800.
[22] S. Peng, R. An, Y. Li, G. Lu, S. Li, Int. J. Hydrogen Energy 37 (2012) 1366–1374.
[23] C. Han, L. Wu, L. Ge, Y. Li, Z. Zhao, Carbon 92 (2015) 31–40.
[24] L. Wu, J. Gong, L. Ge, C. Han, S. Fang, Y. Xin, Y. Li, Y. Lu, Int. J. Hydrogen Energy 41 (2016) 14704–14712.
[25] N. Zhou, L. Polavarapu, N.Y. Gao, Nanoscale 5 (2013) 4236–4241.
[26] Y.Y. Jia, Y.Q. Jiang, J.W. Zhang, L. Zhang, Q.L. Chen, Z.X. Xie, L.S. Zheng, J. Am. Chem. Soc. 136 (2014) 3748–3751.
[27] X. Cao, Y. Han, C. Gao, Y. Xu, X. Huang, M. Willander, N. Wang, Nano Energy 9 (2014) 301–308.
[28] W. Zhang, Y. Li, X. Zeng, S. Peng, Sci. Rep. UK 5 (2015) 10589.
[29] B. Li, H. Cao, J. Yin, Y.A. Wu, J.H. Warner, J. Mater. Chem. 22 (2012) 1876–1883.
[30] K.A.S. Fernando, S. Sahu, Y. Liu, W.K. Lewis, E.A. Guliants, A. Jafariyan, P. Wang, C.E. Bunker, Y.-P. Sun, ACS Appl. Mater. Interfaces 7 (2015) 8363–8376.
[31] X. Qian, D. Yue, Z. Tian, M. Reng, Y. Zhu, M. Kan, T. Zhang, Y. Zhao, Appl. Catal. B 193 (2016) 16–21.
[32] S. Leong, D. Li, K. Hapgood, X. Zhang, H. Wang, Appl. Catal. B 198 (2016) 224–233.
[33] Z. Li, Y. Wu, G. Lu, Appl. Catal. B 188 (2016) 56–64.
[34] M. Xie, S. Duan, Y. Shen, K. Fang, Y. Wang, M. Lin, X. Guo, ACS Energy Lett. 1 (2016) 814–819.
[35] L.J. Zhang, S. Li, B.K. Liu, D.J. Wang, T.F. Xie, ACS Catal. 4 (2014) 3724–3729.
[36] H. Shen, I.-R. Ie, C.-S. Yuan, C.-H. Hung, Appl. Catal. B 195 (2016) 90–103.
[37] J. Zhang, H. Ma, Z. Liu, Appl. Catal. B 201 (2017) 84–91.
[38] Y. Li, H. Wang, S. Peng, J. Phys. Chem. C 118 (2014) 19842–19848.
[39] T. Xiong, M. Wen, F. Dong, J. Yu, L. Han, B. Lei, Y. Zhang, X. Tang, Z. Zang, Appl. Catal. B 199 (2016) 87–95.
[40] A. Han, S. Jin, H. Chen, H. Ji, Z. Sun, P. Du, J. Mater. Chem. A 3 (2015) 1941–1946.
[41] J. Tian, Q. Liu, N. Cheng, A.M. Asiri, X. Sun, Angew. Chem. Int. Ed. 53 (2014) 9577–9581.
[42] H. Yang, Y. Zhang, F. Hu, Q. Wang, Nano Lett. 15 (2015) 7616–7620.
[43] J. Tian, Q. Liu, Y. Liang, Z. Xing, A.M. Asiri, X. Sun, ACS Mater. Interfaces 6 (2014) 20579–20584.
[44] Y. Wang, J. Wu, J. Zheng, R. Xu, Catal. Sci. Technol. 1 (2011) 940–947.
[45] D. Zhao, B. Sun, X. Li, L. Qin, S. Kang, D. Wang, RSC Adv. 6 (2016) 33120–33125.
[46] S. Cao, Y. Chen, C.-J. Wang, X.-J. Lv, W.-F. Fu, Chem. Commun. 51 (2015) 8708–8711.
[47] Z.J. Sun, B.H. Lv, J.S. Li, M. Xiao, P.W. Du, J. Mater. Chem. A 4 (2016) 1598–1602.
[48] J. Tian, Q. Liu, A.M. Asiri, X. Sun, J. Am. Chem. Soc. 136 (2014) 7587–7590.
[49] L. Ye, C. Han, Z. Ma, Y. Leng, J. Li, X. Ji, D. Bi, H. Xie, Z. Huang, Chem. Eng. J. 307 (2017) 311–318.
[50] P. Ye, X. Liu, J. Iocozzia, Y. Yuan, L. Gu, G. Xu, Z. Lin, J. Mater. Chem. A 5 (2017) 8493–8498.